Earth and Planetary Science Letters 408 (2014) 370–377

Contents lists available at ScienceDirect

Earth and Planetary Science Letters

www.elsevier.com/locate/epsl

The Moho beneath western Tibet: Shear zones and eclogitization in the lower crust

Zhongjie Zhang [a,1], Yanghua Wang [b], Gregory A. Houseman [c,*], Tao Xu [a], Zhenbo Wu [a], Xiaohui Yuan [d], Yun Chen [a], Xiaobo Tian [a], Zhiming Bai [a], Jiwen Teng [a]

[a] Institute of Geology and Geophysics, Chinese Academy of Sciences, Beijing, 100029, China
[b] Department of Earth Science and Engineering, Imperial College London, SW7 2AZ, UK
[c] School of Earth and Environment, University of Leeds, LS2 9JT, UK
[d] GFZ German Research Centre for Geosciences, Telegrafenberg, 14473 Potsdam, Germany

ARTICLE INFO

Article history:
Received 11 July 2014
Received in revised form 10 October 2014
Accepted 13 October 2014
Available online 4 November 2014
Editor: A. Yin

Keywords:
Tibetan Plateau
Moho segmentation
receiver functions
crustal thickness
eclogitization
shear zones

ABSTRACT

The Tibetan Plateau is formed by continuing convergence between Indian and Asian plates since ∼50 Ma, involving more than 1400 km of crustal shortening. New seismic data from western Tibet (the TW-80 experiment at 80°E) reveal segmentation of lower crustal structure by the major sutures, contradicting the idea of a mobile lower crust that flows laterally in response to stress variations. Significant changes in crustal structure and Moho depth occur at the mapped major tectonic boundaries, suggesting that zones of localized shear on sub-vertical planes extend through the crust and into the upper mantle. Converted waves originating at the Moho and at a shallower discontinuity are interpreted to define a partially eclogitized layer that extends 200 km north of the Indus–Yarlung Suture Zone, beneath the entire Lhasa block at depths of between 50 and 70 km. This layer is thinner and shallower to the north of the Shiquanhe Fault which separates the northern Lhasa block from the southern part, and the degree of eclogitization is interpreted to increase northward. The segmentation of the Tibetan crust is compatible with a shortening deformation rather than shear on horizontal planes. Unless the Indian-plate mantle lithosphere plunges steeply into the mantle beneath the Indus–Yarlung suture, leaving Indian-plate crust accreted to the southern margin of Tibet, then it too must have experienced a similar shortening deformation.

1. Introduction

Two basic mechanisms have been proposed to explain the high elevation of the Tibetan Plateau: crustal shortening and thickening (Allegre et al., 1984; England and Houseman, 1986), or underthrusting of Indian mantle lithosphere (Ni and Barazangi, 1984; Tilmann et al., 2003; Kumar et al., 2006; Rai et al., 2006; Li et al., 2008). Other processes that may have influenced the evolution of the Tibetan lithosphere and its plateau include lithospheric detachment (Kosarev et al., 1999) or convective thinning (Houseman et al., 1981), underplating (Nábělek et al., 2009), subduction of the Asian lithosphere (Kind et al., 2002), channel flow (Beaumont et al., 2001; Royden et al., 2008) and escape tectonics (Tapponnier et al., 1982; Replumaz and Tapponnier, 2003). These geodynamic processes are interpreted from structural mapping (Yin and Harrison, 2000) and from seismic profiling studies using both controlled source and teleseismic signals, with observations mainly from eastern and central Tibet (e.g., Hirn et al., 1984; Owens and Zandt, 1997; Schulte-Pelkum et al., 2005; Zhao et al., 2010; Mechie and Kind, 2013). Body and surface wave tomography have also provided important constraints on upper mantle structure (Tilmann et al., 2003; Priestley et al., 2006; Ren and Shen, 2008; Li et al., 2008; Replumaz et al., 2012; Liang et al., 2012; Razi et al., 2014).

Contrasting interpretations of how far the Indian plate extends underneath the plateau (Owens and Zandt, 1997; Kosarev et al., 1999; Nábělek et al., 2009; Kind and Yuan, 2010) and whether the lower crust of Tibet has been displaced by channel flow (Beaumont et al., 2001; Royden et al., 2008; Rey et al., 2010) have focused debate on these questions. Using new data from a NS seismic profile across western Tibet, we show that: (1) the entire thickness of the Tibetan crust is segmented by major sub-vertical tectonic structures that separate coherently deformed blocks, and (2) the lower-most 15 to 20 km of the crust beneath southern Tibet is progressively undergoing a phase change which results in a clear

* Corresponding author.
E-mail address: greg@earth.leeds.ac.uk (G.A. Houseman).
[1] Deceased.

http://dx.doi.org/10.1016/j.epsl.2014.10.022

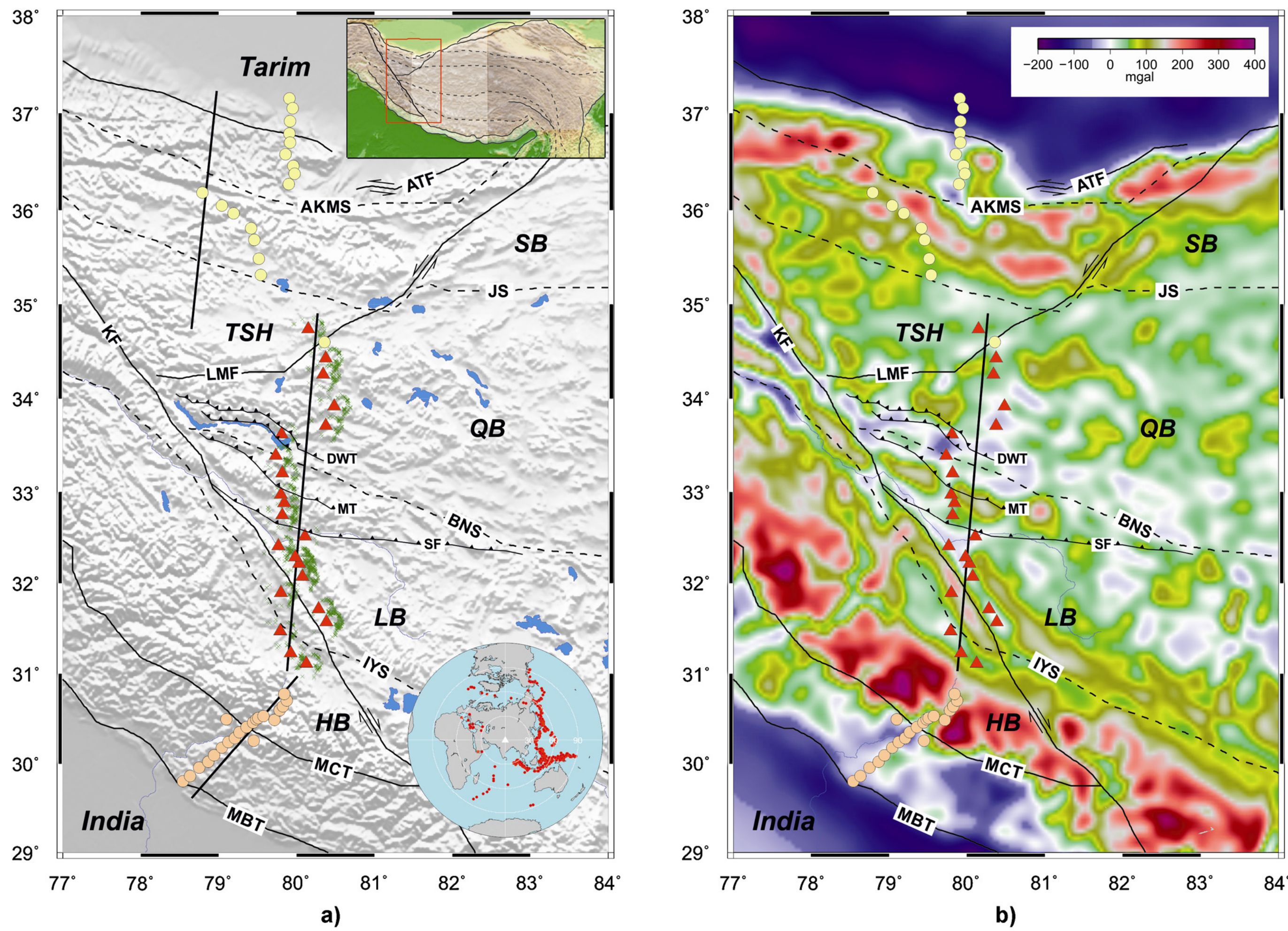

Fig. 1. (a) Map of seismic stations across the western Tibetan Plateau: Red triangles indicate the positions of broadband seismological stations installed for the TW-80 experiment from November 2011 to November 2013. The tan-colored circles show positions of broadband seismological stations used by Caldwell et al. (2013) and Rai et al. (2006) and the yellow circles show stations used in the Sino-French joint project (Wittlinger et al., 2004). The green crosses are the positions of piercing points of PS converted rays at the Moho based on a reference depth of 60 km. Solid lines show projection profiles used by Caldwell et al. (2013), this study, and Wittlinger et al. (2004). Labels denote AKMS: Anyimaqin Kunlun Mustagh Fault; ATF: Altyn Tagh fault; BNS: Bangong–Nujiang suture; DWT: Domar–Wuijiang thrust; HB: Himalaya block; IYS: Indus–Yarlung suture; JS: Jinsha suture; KF: Karakoram fault; LB: Lhasa block, LMF: Longmucuo fault; MBT: Main Boundary Thrust of the Himalayan system; MCT: Main Central Thrust; MT: Mandong–Cuobei thrust; QB: Qiangtang block; SB: Songpan block; SF: Shiquanhe fault; TSH: Tianshuihai block. Top inset: Location of study area in Tibetan Plateau. Bottom inset: Distribution map of events with $Ms > 5.0$ and epicentral distances of 30–90° used in this study. (b) Map of TW-80 station locations and major structural features superposed on a map of Free-air gravity anomalies produced using the EGM2008 gridded gravity dataset (Pavlis et al., 2012). The gravity field has been filtered using a Gaussian filter of width 50 km (as defined by GMT routine *grdfilter*).

south to north variation of the seismic properties of the Lhasa block. This lower crustal layer is bounded above by a discontinuity that is similar to the Moho but less strong and 15 or 20 km less deep. The pair of discontinuities that define this layer is similar to that seen beneath the Hi-CLIMB line 5° further east (Nábělek et al., 2009), but here it extends across the entire Lhasa block. Because the segmentation of the Tibetan crust implies that each of the major crustal blocks is deformed coherently, the Indian mantle lithosphere must be similarly deformed unless it detaches from its crust and descends steeply at the latitude of the Indus–Yarlung suture, contrary to the flat subduction mode interpreted, for example, by Nábělek et al. (2009) or Kind and Yuan (2010).

2. Methods

For the TW-80 experiment (Tibet West, longitude 80°E) an array of broadband seismographs was deployed with average station interval of 15–20 km between November 2011 and November 2013 along a 400 km profile at approximately 80°E, between Zarda in southwest Himalaya and Quanshuigou in northwestern Tibet (for locations see Fig. 1 and Table 1). The TW-80 line crosses the Indus–Yarlung Suture (IYS), the Karakoram fault (KF), the Bangong–Nujiang suture zone (BNS), and other major faults and structures identified on Fig. 1a. During the 24-month observation period from November 2011 to November 2013, 1024 earthquakes with magnitude $Ms > 5.0$, in the distance range 30°–90° provided data that were used in the receiver function analysis. Piercing points of the converted rays at the Moho (assumed 60 km depth) are also shown on Fig. 1a, indicating that most events have back-azimuths between about 20° and 180°.

Individual receiver functions (RFs) were estimated by using time-domain iterative deconvolution of vertical and radial seismograms, as described by Ligorría and Ammon (1999). We obtained 3887 receiver functions for the 22 stations along the profile after eliminating those records for which the Moho *Ps* conversions have a low signal-to-noise (S/N) ratio. A collated section showing the coherence of the individual receiver functions for each station is shown in Fig. 2a.

At each station we processed the available set of receiver functions using the H–κ analysis method of Zhu and Kanamori (2000).